An approach for half-life extension and activity preservation of an anti-diabetic peptide drug based on genetic fusion with an albumin-binding aptide

Daejin Kim, Hyungsu Jeon, Sukyung An, Won Il Choi, Sunghyun Kim, Sangyong Jon

PII: S0168-3659(16)30987-7
DOI: doi: 10.1016/j.jconrel.2017.04.036
Reference: COREL 8781

To appear in: *Journal of Controlled Release*

Received date: 14 October 2016
Revised date: 19 April 2017
Accepted date: 25 April 2017

Please cite this article as: Daejin Kim, Hyungsu Jeon, Sukyung An, Won Il Choi, Sunghyun Kim, Sangyong Jon , An approach for half-life extension and activity preservation of an anti-diabetic peptide drug based on genetic fusion with an albumin-binding aptide. The address for the corresponding author was captured as affiliation for all authors. Please check if appropriate. Corel(2017), doi: 10.1016/j.jconrel.2017.04.036

An approach for half-life extension and activity preservation of an anti-diabetic peptide drug based on genetic fusion with an albumin-binding aptide

Daejin Kim[a,1], Hyungsu Jeon[a,1], Sukyung An[a], Won Il Choi[b], Sunghyun Kim[b,*] and Sangyong Jon[a,*]

[a]KAIST Institute for the BioCentury, Department of Biological Sciences, Korea Advanced Institute of Science and Technology, Daejeon 305-701, Republic of Korea
[b]Korea Institute of Ceramic Engineering and Technology, Jinju 660-031, Republic of Korea

*Corresponding author: Tel: +82-42-350-2634; Fax: +82-42-350-4450; E-mail: syjon@kaist.ac.kr (S. Jon); Tel: +82-55-792-2754; Fax: +82-55-792-2740; E-mail: shkim0519@kicet.re.kr (S. Kim)

[1]These authors contributed equally to this work.

Abstract

Although the peptide, exenatide, has been widely used as a drug for the treatment of type 2 diabetes, its short plasma half-life requires frequent subcutaneous injection, resulting in poor patient compliance in addition to side effects such as infection at the sites of injection. Here, we report a novel long-acting fusion peptide comprising exenatide and a human serum albumin (HSA)-binding aptide. A phage display screen of a library of aptides, yielded an HSA-specific aptide (APT_{HSA}) that bound HSA with a K_d of 188 nM. The recombinant fusion peptide comprising exenatide and APT_{HSA} (exenatide-APT_{HSA}) was expressed in *Escherichia coli* and purified by affinity and size-exclusion chromatography. The resulting exenatide-APT_{HSA} fusion peptide showed glucose-induced insulin secretion activity similar to that of native exenatide when tested *in vitro* using the INS-1 cell line. A pharmacokinetic analysis of exenatide-APT_{HSA} after subcutaneous administration revealed a 4-fold longer plasma half-life (1.3 vs. 0.35 h) compared with exenatide. Furthermore, exenatide-APT_{HSA} showed significantly improved anti-hyperglycemic effects in oral glucose tolerance tests and enhanced hypoglycemic effects compared with exenatide in a *db/db* type 2 diabetes mouse model. These results suggest that the exenatide-APT_{HSA} fusion peptide could be used as a potential anti-diabetic agent for the treatment of type 2 diabetes.

Keywords: Aptides, Exenatide, Human serum albumin, Fusion peptide, GLP-1, Type 2 diabetes

Introduction

Patients with type 2 diabetes have greatly impaired incretin-mediated insulin secretion, mainly owing to decreased secretion of glucagon-like peptide-1 (GLP-1) [1]. The 39-amino acid peptide exenatide, a synthetic version of the hormone exendin-4 found in Gila monster, is a GLP-1 mimetic peptide that has been widely used as an adjunctive therapy to improve glycemic control in diabetes mellitus type 2 patients [2-5]. However, exenatide exhibits a short plasma half-life of ~1.5–4 h in humans [6] owing to its size, which is far smaller than the cutoff for renal excretion, and thus necessitates twice daily subcutaneous injection. In addition to causing side effects, such as infection at the sites of injection, the requirement for frequent injections results in poor patient compliance [7, 8], a limitation that recent efforts have sought to address.

Among the technological solutions that have been investigated for limiting renal clearance of exenatide is fusion of the peptide to large artificial or natural macromolecules, such as polyethylene glycol, XTEN polypeptide, and human serum albumin (HSA) [9-19]. Although such technological approaches have increased the plasma half-life of exenatide up to ~12–38 h, the biological activity of the drug in these conjugates is dramatically reduced (up to 98%) compared to pristine exenatide, limiting further development [20-22]. This significant loss of activity in exenatide fusion conjugates may result from blockage of the peptide's receptor binding site by the larger molecular fusion partners. As alternative approaches, technologies based on albumin-binding peptides (ABP) or albumin-binding domains (ABD) that allow a reversible, non-covalent association with the abundant serum protein have emerged [23, 24]. Such approaches rely on the fact that albumin binds to neonatal Fc receptor (FcRn) in an acidic endosome and is recycled back into the blood circulation at physiological pH, resulting in long circulation half-life in bloodstream [33]. Although such approaches result in a diminished loss of exenatide activity compared with fusions with larger molecular scaffolds, such as XTEN and HSA, concerns remain regarding the potential immunogenicity of ABD and the low-affinity of HSA for ABP. This experience with different fusion partners suggests that a new affinity molecule with a smaller size than ABD and higher affinity than ABP would be a suitable candidate fusion partner for short-acting peptide drugs like exenatide.

Aptides, developed by our group, are a novel class of structure-constrained peptides containing a randomizable binding region and a constant β-hairpin scaffold. By combining this genetic variability with *in vitro* directed evolution strategies, high-specificity and -affinity

peptide binders for various biological targets can be identified from screens of aptide libraries [25-29]. Here, we report a new fusion peptide between exenatide and an HSA-binding aptide (ATP_{HSA}), designated exenatide-ATP_{HSA}. ATP_{HSA} was initially identified by phage display screening, its affinity and specificity for HSA was characterized, and the pharmacokinetics and biological activity of the resulting exenatide-ATP_{HSA} fusion conjugate were examined *in vitro* and *in vivo*. These analyses revealed that exenatide-ATP_{HSA} exhibits an extended half-life while retaining antidiabetic biological activity.

2. Materials and Methods

2.1. Materials

Exenatide (*N*'-HGEGTFTSDLSKQMEEEAVRLFIEWLKNGGPSSGAPPPS-*C*') was synthesized by AnyGen Co. (Gwangju, South Korea). All oligonucleotides for libraries and cloning were purchased from Genotech Inc (Daejeon, South Korea). Female C57BL/6 *db/db* mice (6 wk old) were supplied by the Korean Research Institute of Bioscience and Biotechnology (Daejeon, South Korea) and maintained under pathogen-free conditions in the animal facility at Korea Advanced Institute of Science and Technology (KAIST). Animal experiments were approved by the KAIST Animal Care and Use Committee. Exenatide enzyme-linked immunosorbent assay (ELISA) kits were purchased from Phoenix pharmaceuticals, Inc. (Burlingame, CA, USA) and insulin ELISA kits were purchased from Mercodia (Uppsala, Sweden). The glucose-sensitive pancreatic cell line, INS-1, was cultured in RPMI-1640 medium (Life Technologies, Grand Island, NY, USA) containing 10% heat-inactivated fetal bovine serum (FBS; Life Technologies), 100 units/mL penicillin, and 100 μg/mL streptomycin at 37°C in a humidified 5% CO_2 atmosphere. A One-Touch blood glucose meter (CodeFree) was purchased from SD Biosensor, Inc. (Suwon, South Korea).

2.2. Phage display screening for HSA-binding aptides

An HSA-specific aptide (ATP_{HSA}) was identified using a phage display-based screening method, as described previously [25]. Briefly, HSA was immobilized on 96-well plates (Corning, NY, USA) overnight at 4°C. After incubating phage library pools on HSA-immobilized plates for 1 h at 25°C, unbound phages were removed by washing with phosphate-buffered saline (PBS) containing 0.5% Tween-20 (PBS-T), and bound phages were

eluted with 0.2 M glycine buffer (pH 2.2), followed by immediate neutralization with Tris-HCl (pH 8.8). The eluted phages were amplified in log-phase cultures of *Escherichia coli* ER (New England Biolabs, Ipswich, MA, USA). This biopanning process was reiterated several times using the amplified phages until enrichment of specific phages was achieved. After biopanning, phage ELISAs were carried out. Bound phages were incubated with horseradish peroxidase (HRP)-conjugated anti-M13 antibody (GE Healthcare, Little Chalfont, UK) and then detected by incubation with the chromogenic substrate tetramethylbenzidine (TMB) with subsequent monitoring of absorbance at 450 nm. The sequence of ATP_{HSA} identified by these screens was *N'*-HAHFNFGSWTWENGKWTWKGIWLPAR-*C'*, where the underlined sequence denotes the constant β-hairpin scaffold portion of the aptide structure.

2.3. Specificity assessment of APT_{HSA}

To investigate the specificity of APT_{HSA}, we carried out phage ELISA experiments using HSA and phages displaying APT_{HSA}; negative control protein targets included streptavidin (New England Biolabs, Ipswich, MA, USA), tumor necrosis factor alpha (TNFα; R&D Systems, Minneapolis, US), CD7-Trx, and visfatin (Sigma, St. Louis, MO, USA). All proteins (10 μg/ml in PBS) were immobilized on 96-well plates (Corning, NY, USA) by incubating overnight at 4°C. After blocking with 2% skim milk, phages displaying APT_{HSA} (1×10^8 PFU) were incubated with HSA or control protein for 1 h at 25°C. Then, each plate was washed five times with PBS-T and incubated with HRP-conjugated anti-M13 antibody (GE Healthcare, cat. no. 27-9420-01). The results were visualized by incubating with the TMB substrate (BD Biosciences, Franklin Lakes, NJ, USA) and measuring absorbance at 450 nm.

2.4. Measurement of APT_{HSA} affinity

Affinity of peptides was measured using a BIAcore X instrument (GE Healthcare, Little Chalfont, UK) as described by the manufacturer. Briefly, HSA protein was immobilized on a CM5 chip (GE Healthcare, Little Chalfont, UK). Different concentrations of APT_{HSA} in running buffer (PBS, pH 7.4) were then injected and allowed to interact with HSA at a flow rate of 30 μL/min. All kinetic data for interactions were analyzed using BIAevaluation 3.1 software.

2.5. Preparation of an exenatide-APT_{HSA} fusion peptide

Exenatide-APT_{HSA} was prepared using recombinant DNA technology. A fusion gene for exenatide-APT_{HSA} was generated by concatenating the oligonucleotides encoding exenatide, a linker (GSEGSEGEGGSEGSEGEG), and APT_{HSA}. The gene was amplified by polymerase chain reaction (PCR) using primers obtained from Genotech Inc (Daejeon, South korea). PCR conditions were 30 cycles of 30 s at 95°C, 30 s at 55°C, and 1 min at 72°C. The amplified gene was cloned into the prokaryotic expression vector pET32a (Novagen, Darmstadt, Germany), and the resulting exenatide-APT_{HSA} expression plasmids were transformed into *E. coli* strain BL21 (DE3) (Stratagene, La Jolla, CA, USA). After induction with 1 mM isopropyl β-D-thiogalactopyranoside (IPTG; Sigma) for 20 h at 18°C, the exenatide-APT_{HSA} fusion conjugate was purified using Ni-NTA affinity resin (ELPIS biotech, Daejeon, Korea) following by gel filtration using a Superdex 75 column (Amersham Pharmacia, Little Chalfont, UK) pre-equilibrated with PBS (pH 7.4). The Trx-fusion tag was cleaved by incubating the fusion peptide with enterokinase for 16 h at 20°C, after which exenatide-APT_{HSA} was purified by gel filtration using a Superdex 75 column (Amersham Pharmacia, Little Chalfont, UK) pre-equilibrated with PBS (pH 7.4). Endotoxins were removed using a high capacity endotoxin removal spin column (Pierce, MA, USA).

2.6. *In vitro* biological activity of exenatide-APT_{HSA}

The *in vitro* biological activity of exenatide-APT_{HSA} was determined by measuring insulin secretion by the glucose sensitive pancreatic-cell line, INS-1, after treatment with the fusion peptide. The cells were maintained in complete RPMI-1640 medium (11.1 mM glucose) containing 10% (v/v) FBS, 50 μM 2-mercaptoethanol, 10 mM HEPES, 2 mM glutamine, 1 mM sodium pyruvate, 100 units/mL penicillin and 100 μg/mL streptomycin, and incubated at 37°C in a humidified 5% CO_2 atmosphere. INS-1 cells were incubated in 500 μL of Kreps–Ringer–HEPES (KRH) buffer (11.1 mM glucose) containing exenatide or exenatide-APT_{HSA} (0.1–100 nM) for 1 h, and the levels of insulin released were measured using an insulin ELISA kit.

2.7. *In vivo* pharmacokinetics of exenatide-APT_{HSA}

The pharmacokinetic profiles of exenatide and exenatide-APT_{HSA} that were mixed with HSA (600 μM) through incubation with HSA for 1h were assessed following subcutaneous (s.c.) administration in ICR mice (n = 3) at a dose of 25 nmol/kg. Blood samples were obtained

from the retro-orbital sinus and centrifuged at 700 × g and 4°C for 20 min. The concentration of exenatide or exenatide-APT_{HSA} in the collected supernatants was then measured using an exenatide ELISA kit and calculated based on standard curves for exenatide and exenatide-APT_{HSA}. Pharmacokinetic parameters were estimated by noncompartmental analysis as previously reported [30], where AUC (area under the curve) is calculated using the trapezoidal rule. The terminal-phase elimination half-life ($t_{1/2}$) was calculated as $t_{1/2} = \ln(2)/k_{el}$, where k_{el} (terminal-phase elimination rate constant) was determined from the slope of the terminal portion of the log-concentration-time curve.

2.8. Anti-hyperglycemic efficacy of exenatide-APT_{HSA} in fasted *db/db* mice

The *in vivo* anti-hyperglycemic efficacies of exenatide and exenatide-APT_{HSA} were measured in *db/db* mice using an oral glucose tolerance test (OGTT) [31]. The average body weight and blood glucose levels were the same for all groups. Briefly, mice fasted for 18 h were injected intraperitoneally with saline, exenatide (25 nmol/kg), or exenatide-APT_{HSA} (25 nmol/kg) at t = -60 min. At t = 0 min, 1.0 g/kg of glucose was orally administered, and blood glucose levels were monitored using a One-Touch glucose meter (CodeFree, SD Biosensor, Suwon, South Korea) at set intervals.

2.9. Hypoglycemic efficacy of exenatide-APT_{HSA} in non-fasted *db/db* mice

Hypoglycemic efficacies were evaluated in female *db/db* mice (n = 4/group, 6 wk old) administered intraperitoneally with exenatide (5, 25 nmol/kg), exenateide-APT_{scr} (5 nmol/kg) or exenatide-APT_{HSA} (1, 5, 25 nmol/kg). Mice were kept under non-fasting conditions with free access to water and food until the end of the experiment. A drop of blood was drawn from the tail vein of each mouse at 0, 0.5, 1, 2, 4, 6, 8, 12, 16, 20, 24, 28 h after administration, and blood glucose levels were determined using a One-Touch blood glucose meter.

2.10. Statistical analysis

The data are presented as means ± standard error of the mean (SEM). Statistical analyses were carried out by one-way analysis of variance (ANOVA) using SigmaPlot software (Jandel Scientific, San Rafael, CA, USA), and a *P*-value < 0.05 was considered statistically significant for differences between experimental groups.

3. Results and Discussion

3.1. Selection of an HSA-binding aptide by phage display

Screening of HSA-binding peptides was conducted using phage display of aptide libraries (Fig. 1A and Fig. S1A). Enrichment of phage binding to an HSA-adsorbed surface, detected by ELISA, became apparent after the fourth round of selection (Fig. 1B). Forty-eight HSA-binding phages with signal/background ratios > 3 from output phages of the fifth round were sequenced. A sequence alignment of the selected aptides displayed on the phages revealed a candidate HSA-binding aptide (APT_{HSA}) with a consensus sequence of *N'*-HAHFNFGSWTWENGKWTWKGIWLPAR-*C'* (Fig. S1B). To further investigate the specificity of the candidate phage, we performed phage ELISA experiments. As shown in Figure 1C, the APT_{HSA}-displaying phage showed highly specific binding to HSA, whereas negligible binding was observed for various non-target proteins, including gelatin, streptavidin, CD7, TNFα, and visfatin. Binding properties of the chemically synthesized APT_{HSA} were analyzed using a BIAcore chip onto which HSA was immobilized. APT_{HSA} exhibited an association rate constant (k_α) of ~1.23×10^5 $M^{-1}s^{-1}$ and a dissociation rate constant (k_d) of 2.33×10^2 s^{-1}, yielding a dissociation constant (K_d) of ~188 nM (Fig. 1D). The affinity of APT_{HSA} for HSA is higher than that of other albumin-binding peptides reported to date.

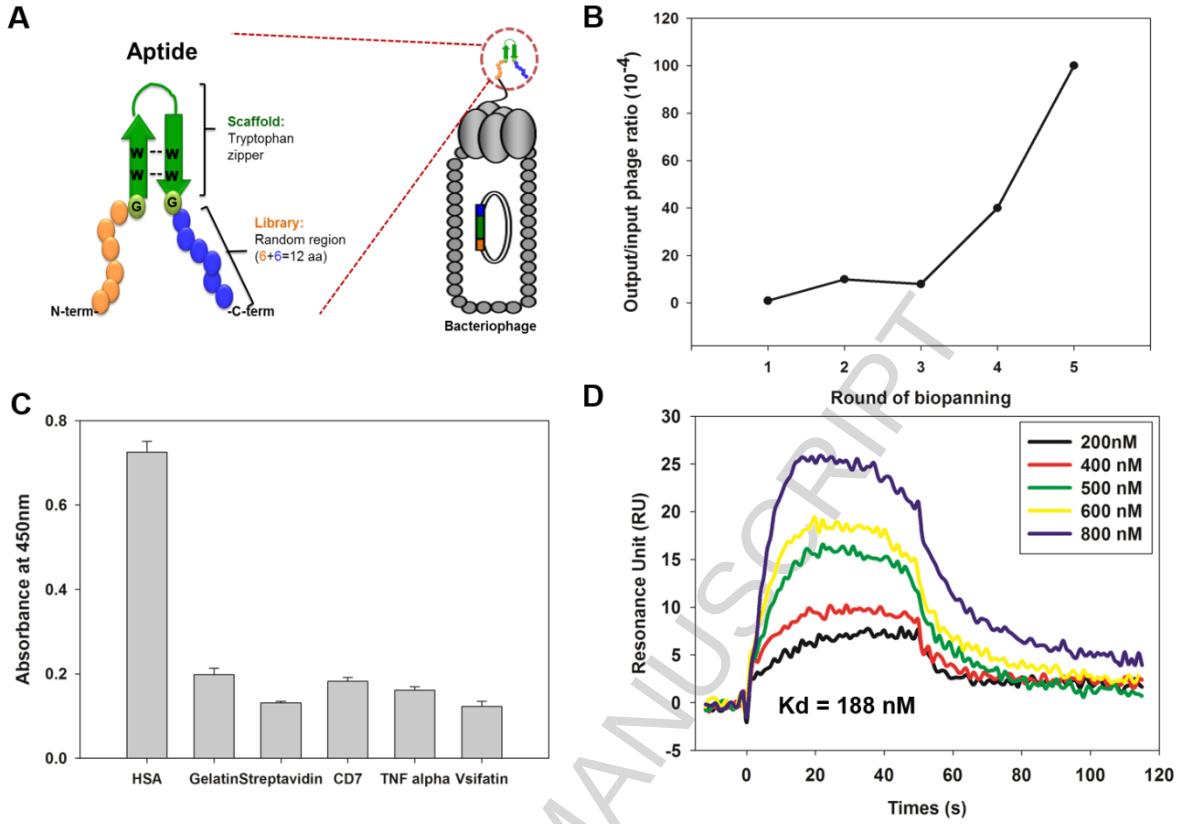

Fig. 1. Screening and identification of HSA-specific peptides. (A) Schematic depiction of aptide molecules. (B) Output/input phage ratios after one, two, three, four and five rounds of phage library screening for HSA. (C) Specificity of APT_{HSA}. Phage ELISAs using a phage displaying the APT_{HSA} sequence against various proteins (HSA, gelatin, streptavidin, CD7, TNFα and visfatin). (D) Surface plasmon resonance sensorgrams and kinetic binding parameters of APT_{HSA} for HSA.

3.2. Design and preparation of the exenatide-APT_{HSA} fusion peptide

As shown in Figure 2A, the C-terminal part of exenatide was connected to the N-terminal part of APT_{HSA} using a long (18-mer) linker to minimize loss of peptide drug activity (Supplementary Table 1.) [32]. The fusion peptide, exenatide-APT_{HSA}, was prepared biologically through protein expression in a bacterial system. To this end, a cDNA for exenatide-linker-APT_{HSA} was constructed and cloned into the pET32a prokaryotic expression vector, which was then used to transform *E. coli* strain BL21(DE3) (Fig. 2A). After expression and purification by sequential affinity chromatography, a fusion protein of thioredoxin-exenatide-APT_{HSA} with a molecular weight of 27 kDa was obtained with 95% purity (Fig. 2B). Finally, the fusion protein was treated with enterokinase, resulting in

cleavage between thioredoxin and exenatide to yield the desired ~9.5 kDa fusion peptide (95% purity) after size exclusion chromatography (Fig. 2C). Next, the stability and toxicity of the purified exenatide-APT_{HSA} fusion peptide were evaluated under the *in vitro* conditions. No degradation was observed for exenatide-APT_{HSA} upon incubation in the presence of serum up to 8 h (Fig. S2). In addition, as shown in Figure S3, exenatide-APT_{HSA} did not affect cell viabilities of both HUVEC and INS-1 cells up to the concentration of 1 μM. Furthermore, unlike E. coli-treated red blood cells, no hemolysis was observed from the fusion peptide-treated group (Fig. S3). Collectively, these results suggest that exenatide-APT_{HSA} has good biocompatibility and stability to be used as an anti-diabetic peptide like pristine exenatide in the *in vivo*.

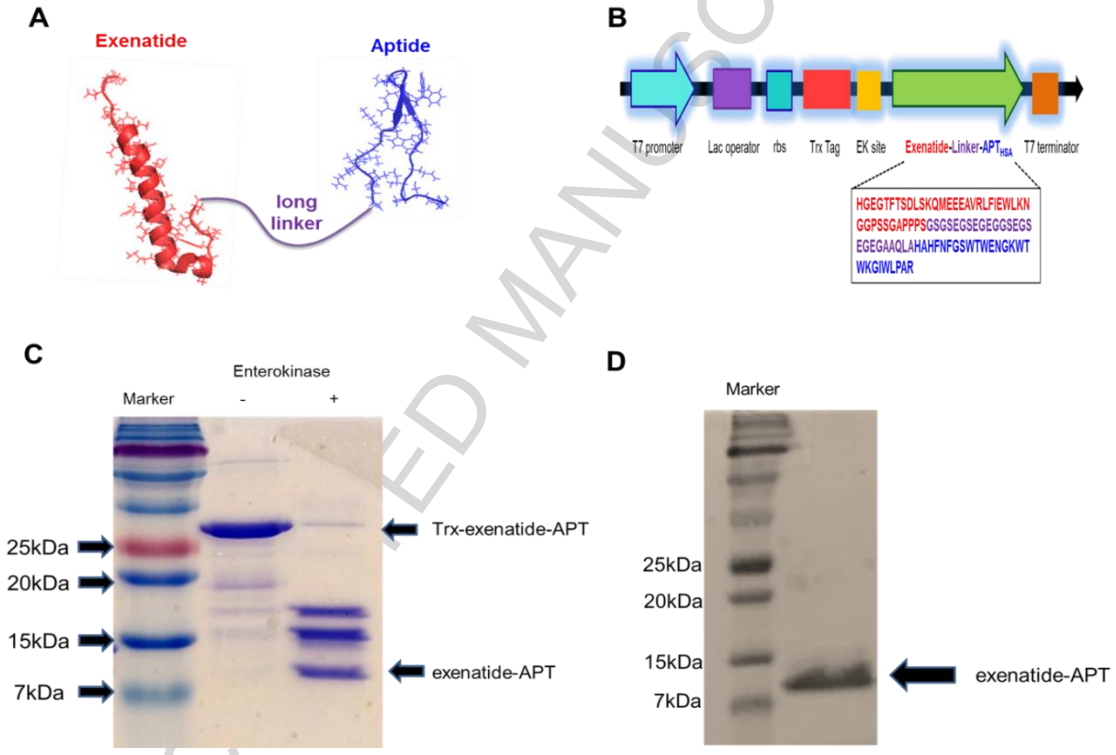

Fig. 2. Preparation of the exenatide-APT_{HSA} fusion peptide. (A) Schematic depiction of the exenatide-ATP_{HSA} fusion peptide based on the NMR structures of exenatide and an aptide [25, 32]. (B) Exenatide-APT_{HSA} cDNA construct cloned into the pET32a vector. (C) SDS-PAGE analysis of Trx-exenatide-APT_{HSA} after treatment with enterokinase and (D) the separated exenatide-APT_{HSA} by size-exclusion chromatography.

3.3. *In vitro* binding and biological activity of exenatide-APT_{HSA}

We examined whether exenatide-APT_{HSA} retains its binding ability to HSA and besides, does

not affect the FcRn-mediated recycling pathway of HSA. Exenatide-APT$_{HSA}$ showed high binding to HSA, but did not bind to control streptavidin, suggesting its specificity (Figure 3A). In addition, it showed binding activity to HSA that was pre-bound to FcRn at pH 6.0 (Figure S4A). Since the binding of exenatide-APT$_{HSA}$ to HSA may inhibit the natural binding mode of HSA to FcRn receptor and the subsequent pH-dependent recycling pathway, we further examined the possibility. As shown in Figure S4 B and C, the binding of HSA to human FcRn receptor was not inhibited in the presence of exenatide-APT$_{HSA}$, suggesting a non-competitive binding mode with FcRn against HSA. Furthermore, there was no difference in the binding of exenatide-APT$_{HSA}$ to HSA between two pHs, pH 7.4 and pH 6.0, respectively. Collectively, these findings suggest that exenatide-APT$_{HSA}$ retains its specific binding activity for HSA and may not interfere the natural FcRn-mediated recycling pathway of HSA.

We next examined whether the fusion peptide is able to retain the biological activity of exenatide, which acts as a GLP-1 agonist to stimulate insulin secretion by pancreatic β-cells. For these experiments, we used INS-1 pancreatic β-cells, which have been previously used in studies of glucose-induced insulin secretion [31]. The cells treated with exenatide-APT$_{HSA}$ (0.1, 1, 10, 100 nM) in the presence of glucose (11.1 mM) secreted insulin in a concentration-dependent manner with slightly lower amounts than the exenatide-treated cells (Fig. 3B). Importantly, exenatide-APT$_{HSA}$ retained nearly 90% of the biological activity of the original exenatide. This value for exenatide-APT$_{HSA}$ is highly impressive considering that previous exenatide fusions tested (exenatide-ABD and exenatide-ABP) preserved only ~10% of the biological activity of the original exenatide [21]. This result might be attributable to the presence of the long, flexible linker inserted between exenatide and the aptide, which may allow exenatide to freely bind to the GLP-1 receptor without steric hindrance.

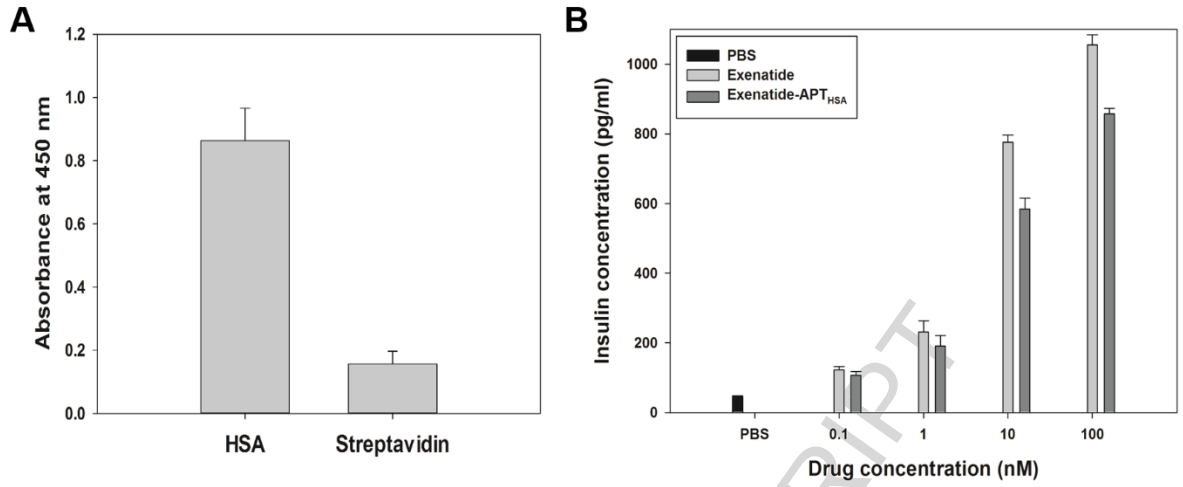

Fig. 3. Functionality evaluation of exenatide-APT$_{HSA}$. (A) HSA-binding activity of exenatide-APT$_{HSA}$. Exenatide-APT$_{HSA}$ was allowed to bind on HSA- or control streptavidin-coated 96-well plates. After washing, the bound exenatide-APT$_{HSA}$ was detected by ELISA using an anti-exenatide antibody. (B) Insulinotropic activities of exenatide and exenatide-APT$_{HSA}$ toward INS-1 insulinoma cells. INS-1 cells were incubated in 500 μL of Kreps–Ringer–HEPES buffer containing 11.1 mM of glucose with exenatide or exenatide-APT$_{HSA}$ for 1 h, and the resulting insulin release was measured using an insulin ELISA kit. Results are presented as means ± SEM (n = 6).

3.4. Pharmacokinetic analysis of exenatide-APT$_{HSA}$

The pharmacokinetics of exenatide-APT$_{HSA}$ in blood was determined and compared with that of exenatide after subcutaneous injection of each compound into ICR mice. The amount of exenatide in blood was quantified using an ELISA kit based on reference to a standard curve prepared by spiking blood with known concentrations of exenatide. As shown in Figure 4A, exenatide was rapidly removed from the circulation, exhibiting a circulating half-life ($t_{1/2}$) of ~0.35 h, whereas exenatide-APT$_{HSA}$ showed a $t_{1/2}$ of ~1.3 h, indicative of ~4-fold slower clearance in the blood. Moreover, the area-under-the curve (AUC_{0-t}) of exenatide-APT$_{HSA}$ was approximately 5-fold larger than that of exenatide (1,060 *versus* 210 ng/ml·h), demonstrating its potential for use as a long-acting platform. We speculate that this extended half-life of exenatide-APT$_{HSA}$ in mouse might be resulted from following two modes of action. First, the size of the fusion peptide-HSA complex increases significantly (~76 kDa) above the renal clearance threshold, leading to the increase of the half-life. Second, the

interaction between HSA and mouse FcRn receptor might also contribute to the half-life increase of exenatide-APT$_{HSA}$ via the receptor-mediated recycling pathway. However, it has been shown that HSA binds to mouse FcRn receptor with approximately 100-fold weaker than endogenous mouse serum albumin [34] and the half-life of HSA in wild type mouse is only marginally increased than in FcRn knockout mouse [35], suggesting the limitation of our experimental settings in this PK study. As such, we expect that more precise PK profile of the fusion protein could be obtained in the human FcRn expressing mouse model [35-37].

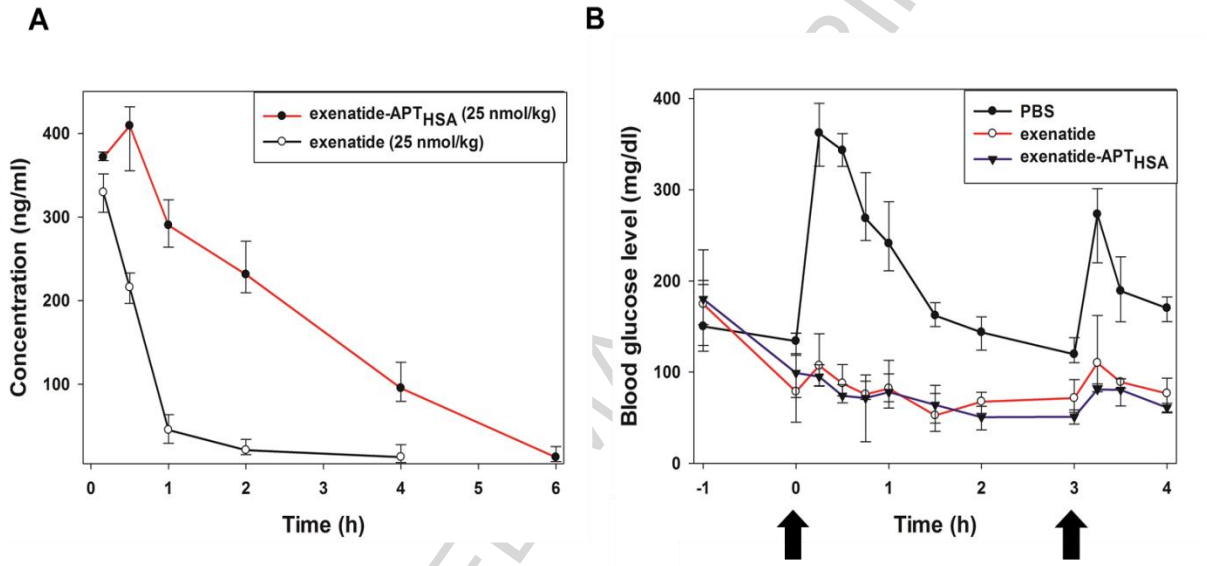

Fig 4. Characteristics of exenatide-APT$_{HSA}$ *in vivo*. (A) Pharmacokinetic profiles of exenatide (s.c.) ad exenatide-APT$_{HSA}$ (s.c.) in ICR mice. Results are presented as means±SEM (n = 3/group). (B) Anti-hyperglycemic activities of exenatide and exenatide-APT$_{HSA}$ (1 g/kg, i.p.) as determined by two consecutive OGTTs in type 2 diabetic *db/db* mice fasted for 18 h. Arrows denote glucose challenges times.

3.5. Anti-hyperglycemic activities of exenatide and exenatide-APT$_{HSA}$ in fasted *db/db* mice

The *in vivo* biological activities of exenatide and exenatide-APT$_{HSA}$ were first assessed by comparing their anti-hyperglycemic efficacies in OGTTs in type 2 *db/db* mice. Mice were divided into three treatment groups: PBS (control), exenatide, and exenatide-APT$_{HSA}$. Each compound was administered intraperitoneally at a dose of 25 nmol/kg, 60 min before oral injection of glucose, then changes in blood glucose levels were measured over time (Fig. 4B). Whereas the PBS control group showed a rapid increase in glucose level followed by a slow

ndecrease, both exenatide and exenatide-APT_{HSA} groups at an equal dose effectively cleared glucose from the bloodstream, showing similar anti-hyperglycemic activity (Fig. 4B). These results clearly indicate that the fusion peptide retains biological activity similar to that of exenatide.

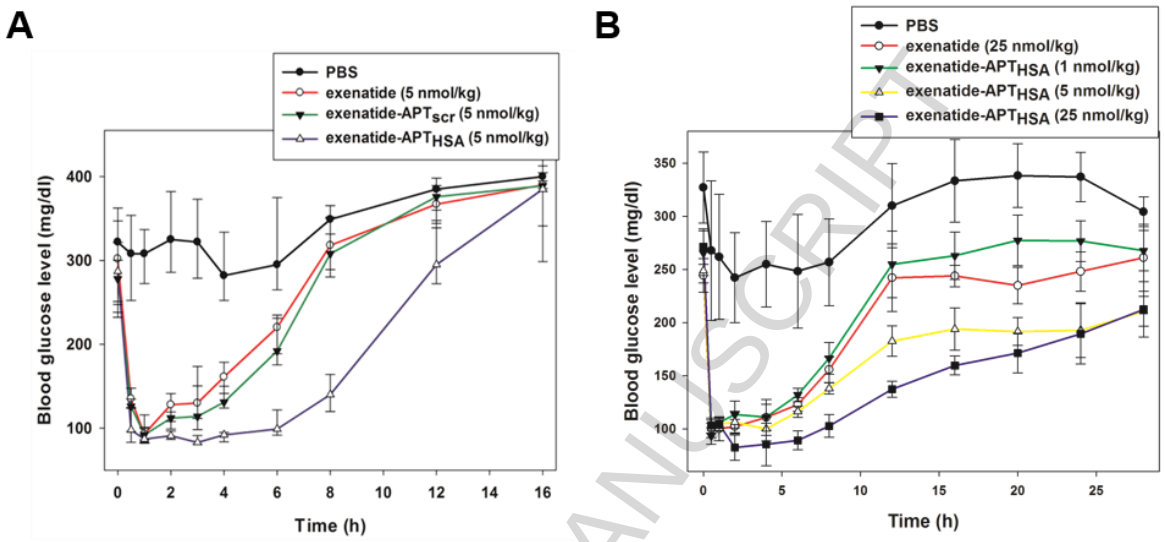

Fig. 5. Hypoglycemic activities of exenatide and exenatide-APT_{HSA} in non-fasting *db/db* mice (A) at single dose and (B) at doses of 1, 5 and 25 nmol/kg.

3.6. Hypoglycemic effect of exenatide-APT_{HSA} in non-fasted *db/db* mice

The hypoglycemic effect of exenatide-APT_{HSA} (5 nmol/kg) was evaluated in non-fasted type 2 diabetic *db/db* mice and compared with that of exenatide or exenatide-APT_{scr}, a fusion peptide containing a non-relevant scrambled aptide sequence. As shown in Figure 5A, there was no significant difference in the nadir of glucose level (~80 mg/dL) reached by all three groups; however, mice treated with exenatide-APT_{HSA} showed a significantly delayed rebound time from this low point (increased duration of action) compared with mice treated with exenatide or exenatide-APT_{scr} (~12 h *versus* ~7 h). The similar hypoglycemic effect of exenatide-APT_{scr} compared with that of exenatide supports the conclusion that the albumin-binding element in exenatide-APT_{HSA} plays a crucial role in extending the biological activity of exenatide in blood. We next examined the dose dependency of this hypoglycemic effect. As shown in Figure 5B, the rebound time from the nadir (~80 mg/dL) to the diabetic level (> ~250 mg/dL) of blood glucose significantly increased with rise in the dose of exenatide-APT_{HSA} (1, 5 and 25 nmol/kg). Noticeably, the hypoglycemic profile of exenatide-APT_{HSA} at a dose of 1 nmol/kg was comparable to that of 25 nmol exenatide/kg; moreover, exenatide-

APT_{HSA} at a dose of 25 nmol/kg could maintain the blood glucose below 150 mg/dL for far longer time period than free exenatide at the same dose (~16 h versus ~7 h) (Fig. 5B). $AUC_{0\text{-}24h}$ values revealed that exenatide-APT_{HSA} had ~57% greater anti-diabetic effect than exenatide at a dose of 25 nmol/kg (3,920 versus 2,497 mg·h/mL relative to PBS-treated control) (Fig. S5). This result clearly indicates that exenatide-APT_{HSA} can extend the therapeutic effect of exenatide more than at least 2-fold in a type 2 diabetic mouse model.

4. Conclusions

In this proof-of-concept study, we developed a novel fusion peptide between exenatide and an HSA-binding aptide (APT_{HSA}) as a means for extending the half-life and minimizing the biological activity loss of this existing antidiabetic peptide drug. Phage display of aptide libraries enabled us to screen and select APT_{HSA}, which showed higher binding affinity compared with previously reported HSA-binding peptides. Moreover, unlike other fusion proteins or peptides between exenatide and albumin-binding molecules, the genetic fusion with APT_{HSA} incorporating a long linker maximally preserved the biological activity of exenatide *in vitro* as well as *in vivo*. Furthermore, the exenatide-APT_{HSA} fusion peptide showed significantly improved pharmacokinetic and pharmacodynamics characteristics compared with exenatide in a *db/db* type 2 diabetes mouse model. Taken together, our results suggest that the strategy employing fusion with HSA-specific aptides to develop a long-acting exenatide derivative described here could be also applied to other important peptide- or protein-based biotherapeutics. However, before advancing into clinical applications, exact pharmacokinetics of exenatide-APT_{HSA} should be assessed by using state-of-art animal models such as human FcRn-expressing transgenic mouse. Furthermore, the affinity of the present APT_{HSA} for serum HSA will need to be significantly improved to further increase blood circulation time. We may be able to address these issues in the near term through an affinity-maturation process conducted using focused-libraries based on the first hit, APT_{HSA} and animal experiments using human FcRn-expressing mouse models.

Acknowledgments

This work was supported by a Global Research Laboratory (2015045887) through the National Research Foundation of Korea, funded by the Ministry of Science, ICT, and Future Planning.

References

[1] D.J. Drucker, Biologic actions and therapeutic potential of the proglucagon-derived peptides, Nat. Clin. Pract. Endocrinol. Metab. 1 (2005) 22–31.

[2] R.S. Cvetkovic, G.L. Plosker, Exenatide: a review of its use in patients with type 2 diabetes mellitus, Drugs, 67 (2007) 935–954.

[3] C. Triplitt, E. Chiquette, Exenatide: from the Gila monster to the pharmacy, J. Am. Pharm. Assoc. 46 (2006) 44–55.

[4] J. Eng, W.A. Kleinman, L. Singh, G. Singh, J.P. Raufman, Isolation and characterization of exendin-4, an exendin-3 analogue, from Heloderma suspectum venom. Further evidence for an exendin receptor on dispersed acini from guinea pig pancreas, J. Biol. Chem. 267 (1992) 7402–7405.

[5] R. Gentilella, C. Bianchi, A. Rossi, C.M. Rotella, Exenatide: a review from pharmacology to clinical practice, Diabetes. Obes. Metab. 11 (2009) 544–556.

[6] N. Gong, A.N. Ma, L.J. Zhang, X.S. Luo, Y.H. Zhang, M. Xu, Y.X. Wang, Site-specific PEGylation of exenatide analogues markedly improved their glucoregulatory activity, Br. J. Pharmacol. 163 (2011) 399–412.

[7] B.R. Gedulin, P.A. Smith, C.M. Jodka, K. Chen, S. Bhavsar, L.L. Nielsen, D.G. Parkes, A.A. Young, Pharmacokinetics and pharmacodynamics of exenatide following alternate routes of administration, Int. J. Pharm. 356 (2008) 231–238.

[8] L. Simonsen, J.J. Holst, C.F. Deacon, Exendin-4, but not glucagon-like peptide-1, is cleared exclusively by glomerular filtration in anaesthetised pigs, Diabetologia 49 (2006) 706–712.

[9] B. Meibohm, H. Zhou, Characterizing the impact of renal impairment on the clinical pharmacology of biologics, J. Clin. Pharmacol. 52 (2012) 54S–62S.

[10] R. Clark, K. Olson, G. Fuh, M. Marian, D. Mortensen, G. Teshima, S. Chang, H. Chu, V. Mukku, E. Canova-Davis, T. Somers, M. Cronin, M. Winkler, J.A. Wells, Long-acting growth hormones produced by conjugation with polyethylene glycol, J. Biol. Chem. 271 (1996) 21969–21977.

[11] J.M. Harris, R.B. Chess, Effect of pegylation on pharmaceuticals, Nat. Rev. Drug. Discov. 2 (2003) 214–221.

[12] L.S. Lee, C. Conover, C. Shi, M. Whitlow, D. Filpula, Prolonged circulating lives of single-chain Fv proteins conjugated with polyethylene glycol: a comparison of

conjugation chemistries and compounds, Bioconjug. Chem. 10 (1999) 973–981.

[13] Y. Yamamoto, Y. Tsutsumi, Y. Yoshioka, T. Nishibata, K. Kobayashi, T. Okamoto, Y. Mukai, T. Shimizu, S. Nakagawa, S. nagata, T. Mayumi, Site-specific PEGylation of a lysine-deficient TNF-alpha with full bioactivity, Nat. Biotechnol. 21 (2003) 546–552.

[14] P. Bailon, A. Palleroni, C.A. Schaffer, C.L. Spence, W.J. Fung, J.E. Porter, G.K. Ehrlich, W. Pan, Z.X. Xu, M.W. Modi, A. Farid, W. Berthold, M. Graves, Rational design of a potent, long-lasting form of interferon: a 40 kDa branched polyethylene glycol-conjugated interferon alpha-2a for the treatment of hepatitis C, Bioconjug Chem. 12 (2001) 195-202.

[15] V. Schellenberger, C.W. Wang, N.C. Geething, B.J. Spink, A. Campbell, W. To, M.D. Scholle, Y. Yin, Y. Yao, O. Bogin, J.L. Cleland, J. Silverman, W.P. Stemmer, A recombinant polypeptide extends the in vivo half-life of peptides and proteins in a tunable manner, Nat. Biotechnol. 27 (2009) 1186–1190.

[16] S.E. Alters, B. McLaughlin, B. Spink, T. Lachinyan, C.W. Wang, V. Podust, V. Schellenberger, W.P. Stemmer, GLP2–2G-XTEN: a pharmaceutical protein with improved serum half-life and efficacy in a rat Crohn's disease model, PLoS One 7 (2013) e50630.

[17] G.M. Subramanian, M. Fiscella, A. Lamouse-Smith, S. Zeuzem, J.G. McHutchison, Albinterferon alpha-2b: a genetic fusion protein for the treatment of chronic hepatitis C, Nat. Biotechnol. 25 (2007) 1411-1419.

[18] L.L. Baggio, Q. Huang, T.J. Brown, D.J. Drucker, A recombinant human glucagon-like peptide (GLP)-1-albumin protein (albugon) mimics peptidergic activation of GLP-1 receptor-dependent pathways coupled with satiety, gastrointestinal motility, and glucose homeostasis, Diabetes 53 (2004) 2492–2500.

[19] S. Schulte, Half-life extension through albumin fusion technologies, Thromb. Res. 124 (2009) S6-S8.

[20] F. Selis, R. Schrepfer, R. Sanna, S. Scaramuzza, G. Tonon, S. Dedoni, P. Onali, G. Orsini, S. Genovese, Enzymatic mono-pegylation of glucagon-like peptide 1 towards long lasting treatment of type 2 diabetes, Results Pharma. Sci. 2 (2012) 58-65.

[21] V.N. Podust, B.C. Sim, D. Kothari, L. Henthorn, C. Gu, C.W. Wang, B. McLaughlin, V. Schellenberger, Extension of in vivo half-life of biologically active peptides via chemical conjugation to XTEN protein polymer, Protein Eng. Des. Sel. 26 (2013) 743-753.

[22] Y.M. Kim, S.M. Lee, H.S. Chung, Novel AGLP-1 albumin fusion protein as a long-lasting agent for type 2 diabetes, BMB Rep. 46 (2013) 606-610.

[23] O.E. Levy, C.M. Jodka, S.S. Ren, L. Mamedova, A. Sharma, M. Samant, L.J. D'Souza,

C.J. Soares, D.R. Yuskin, L.J. Jin, D.G. Parkes, K. Tatarkiewicz, S.S. Ghosh, Novel exenatide analogs with peptidic albumin binding domains: potent anti-diabetic agents with extended duration of action, PLoS One 9 (2014) e87704.

[24] J. Lindgren, E. Refai, S.V. Zaitsev, L. Abrahmsén, P.O. Berggren, A.E. Karlström, A GLP-1 receptor agonist conjugated to an albumin-binding domain for extended half-life, Biopolymers 102 (2014) 252-259.

[25] S. Kim, D. Kim, H.H. Jung, I.H. Lee, J.I. Kim, J.Y. Suh, S. Jon, Bio-inspired design and potential biomedical applications of a novel class of high-affinity peptides, Angew. Chem. Int. Ed. Engl. 51 (2012) 1890-1894.

[26] D.H. Jo, S. Kim, D. Kim, J.H. Kim, S. Jon, J.H. Kim, VEGF-binding aptides and the inhibition of choroidal and retinal neovascularization, Biomaterials 35 (2014) 3052-3059.

[27] D. Kim, I.H. Lee, S. Kim, M. Choi, H. Kim, S. Ahn, P.E. Saw, H. Jeon, Y. Lee, S. Jon, A specific STAT3-binding peptide exerts antiproliferative effects and antitumor activity by inhibiting STAT3 phosphorylation and signaling, Cancer Res. 74 (2014) 2144-2151.

[28] J. Park, S. Park, S. Kim, I.H. Lee, P.E. Saw, K. Lee, Y.C. Kim, Y.J. Kim, O.C. Farokhzad, Y.Y. Jeong, S. Jon, HER2-specific aptide conjugated magneto-nanoclusters for potential breast cancer imaging and therapy, J. Mater. Chem. B 1 (2013) 4576-4583.

[29] S. Park, Y.J. Kim, S. Jon, A high-affinity peptide for nicotinic acetylcholine receptor-α1 and its potential use in pulmonary drug delivery, J. Control. Release. 192 (2014) 141-147.

[30] W.I. Choi, N. Kamaly, L. Riol-Blanco, I.H. Lee, J. Wu, A. Swami, C. Vilos, B. Yameen, M. Yu, J. Shi, I. Tabas, U.H. von Andrian, O.C. Farokhzad, A solvent-free thermosponge nanoparticle platform for efficient delivery of labile proteins, Nano Letter 14 (2014) 6449-6455.

[31] C.H. Jin, S.Y. Chae, S. Son, T.H. Kim, K.A. Um, Y.S. Youn, S. Lee, K.C. Lee, A new orally available glucagon-like peptide-1 receptor agonist, biotinylated exendin-4, displays improved hypoglycemic effects in db/db mice, J. Control. Release 133 (2009) 172–177.

[32] J.W. Neidigh, R.M. Fesinmeyer, K.S. Prickett, N.H. Andersen, Exendin-4 and glucagon-like-peptide-1: NMR structural comparisons in the solution and micelle-associated states, Biochemistry 40 (2001) 13188-13200.

[33] D. Sleep, J. Cameron, L.R. Evans, Albumin as a versatile platform for drug half-life extension. Bba-Gen Subjects, 1830 (2013) 5526-5534.

[34] J.T. Andersen, M.B. Daba, G. Berntzen, T.E. Michaelsen, I. Sandlie, Cross-species binding analyses of mouse and human neonatal Fc receptor show dramatic differences in

immunoglobulin G and albumin binding. The Journal of biological chemistry, 36 (2010) 4826-4836.

[35] D.C. Roopenian, B.E. Low, G.J. Christianson, G. Proetzel, T.J. Sproule, M.V. Wiles, Albumin-deficient mouse models for studying metabolism of human albumin and pharmacokinetics of albumin-based drugs. mAbs, 7 (2015) 344-351.

[36] D.C. Roopenian, G.J. Christianson, T.J. Sproule, Human FcRn transgenic mice for pharmacokinetic evaluation of therapeutic antibodies. Methods in molecular biology, 602 (2010) 93-104.

[37] G. Proetzel, D.C. Roopenian, Humanized FcRn mouse models for evaluating pharmacokinetics of human IgG antibodies. Methods, 65 (2014) 148-153.

Graphical abstract